Power System Technology
ISSN:1000-3673

Received: 06-04-2024 Revised: 15-05-2024 Accepted: 28-06-2024

Examining the Application of Neural Networks in Predicting Temperature and Solar Cell Power

Milad Mohebbi[1],Abolfazl Rafat[2*],Ghorban Rafat[3]

[1]Division of Mechatronics Engineering, Faculty of Mechanical Engineering, University of Tabriz, 29 Bahman Blvd, Tabriz 51666 14761, Iran
Miladmhbbi7@gmail.com

[2]Lecturer at Bojnoord University, Shirvan College of Agriculture, Shirvan, Iran
rafat.articleabolfazl@gmail.com

[3]Education North Khorasan, Shirvan city, Iran

Abstract:

Cost-effective and efficient engineering of solar cells, in addition to creative design, necessitates a detailed examination of the physics involved in solar energy absorption. Solar energy does not operate at night without storage means such as batteries, and cloudy weather can render this technology unreliable during the day. Since solar cells are used to convert light into electricity, they must be composed of materials efficient in light absorption. Like any other power generation source, solar cells face challenges, including reduced output power with increasing cell surface temperature. With each degree rise in temperature, efficiency can decrease by up to 54.0%, highlighting the importance of addressing and implementing solutions to this issue.

This study explores different specifications of solar cells after a general overview and modeling. It investigates methods for estimating solar cell temperature using ambient temperature and solar radiation, comparing them with a proposed neural network approach. If the neural network can achieve lower error rates than the desired thresholds, it would offer advantages over mathematical estimators mentioned in the literature. Additionally, this neural network demonstrates the capability to predict future solar cell temperatures, unlike instantaneous mathematical estimators for temperature and radiation.

Keywords: Solar cells, temperature estimation methods, neural networks, maximum power point tracking

Introduction:

Solar energy, an infinite source of energy, is completely free from environmental pollution. It easily compensates for energy derived from non-renewable sources such as fossil fuels and underground oil reserves. In recent years, solar energy has experienced extraordinary growth due

Power System Technology
ISSN:1000-3673
Received: 06-04-2024 Revised: 15-05-2024 Accepted: 28-06-2024

to technological advancements leading to cost reductions and governmental policies supporting the development and use of renewable energies. Solar cells have been widely utilized in various applications due to their environmental cleanliness and direct conversion of solar energy into electricity. Silicon-based solar cells are prevalent but costly to produce, whereas polymer solar cells offer flexibility and lower manufacturing costs. Indium tin oxide (ITO) is the most important and practical material used as an electrode in polymer solar cells (Sadeghi et al., 2023).

The increasing global demand for energy, alongside population growth, has escalated the global need for energy. This trend has sparked a global movement towards new energy sources, particularly green energies with minimal environmental impact, spearheaded by solar energy. On the other hand, a crucial prerequisite for the advancement of solar cells is the reduction in production costs and the scaling-up of production speed (Raei et al., 2023). Therefore, this paper explores the application of neural networks in predicting temperature and power output of solar cells.

Theoretical Foundations and Research Methodology:

Modeling of Photovoltaic Modules

A photovoltaic module itself is composed of smaller units known as photovoltaic cells. Therefore, to examine the structure of a PV module, it is necessary to first understand the photovoltaic cell. Typically, a solar cell is represented as an equivalent circuit of a single diode, as shown in Figure 4.

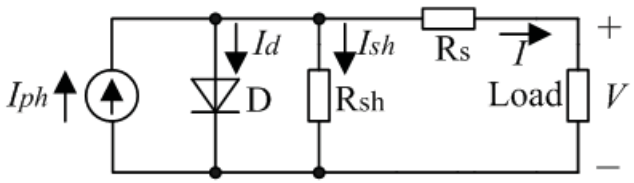

Figure 4: Single Diode Equivalent Circuit in a Solar Cell [41]

Iph represents the photocurrent generated in the PV cell, which is proportional to different levels of irradiance. I is the output current of the PV cell, Id is the diode current, and I5 is the reverse saturation current of the solar cell. V denotes the output voltage of the PV cell. Rsh and Rs are respectively the parallel and series resistances, with Rsh being very large and Rs being very small. When several solar cells are connected in series, they are denoted by ns, and if connected in parallel, they are denoted by np.

The above parameters are derived from the following equations:

Power System Technology
ISSN:1000-3673
Received: 06-04-2024 Revised: 15-05-2024 Accepted: 28-06-2024

$$I_m = n_p n_{ph} - n_p I_o \left[\exp \frac{q\frac{v}{n_s}+IR_s}{nk_t} - 1\right] - \frac{\frac{v}{n_s}+IR_s}{R_{sh}} \quad (1)$$

Here are the parameters obtained from the equations above:

$$I_O = I_{do}\left[\exp \frac{T}{T_{ref}}\right]^3 exp\left[\frac{qE_g}{n_k}\left(\frac{1}{T_{ref}} - \frac{1}{T}\right)\right] \quad (2)$$

$$I_{ph} = I_{sh}\left(\frac{S}{1000}\right) + C_T\,(T - T_{ref}) \quad (3)$$

These formulas relate to electron charge \(q \), with a value of $q = 1.6022 * 10^{-19}\,C$ and k the Boltzmann constant $K = JK^{-1}$, which is $1.3807 * 10^{-23}$Additionally, n_k represents the diode ideality factor, $C_t$denotes the temperature coefficient of the reverse diode current, and S refers to different levels of solar irradiance in units ofw/m^2. $T_{ref}$is the reference temperature, and $T$is the ambient temperature in Kelvin. Bandgap energy $E_g$for silicon typically ranges between $ev\ (1-3)$.

Photovoltaic cells produce low levels of voltage and current, which are not suitable for most applications. Therefore, cells are connected in series and parallel configurations to increase voltage and current levels, forming what is known as a photovoltaic module.

Manufacturers assemble modules using parallel branches of $N_{PM}$where each branch consists of N_{SM} cells connected in series.

There are two main approaches to model photovoltaic modules:

1. Electrical method: Involves replacing each photovoltaic cell with an electrical model. This method is less commonly used due to its difficulty in providing accurate results and simulation challenges.

2. Mathematical modeling method: Invented by Lorenz in 411, this method uses manufacturer's catalog data to create the model. Its main advantage lies in the ability to create the model solely based on available information and data.

The current I^M of a photovoltaic module under operating conditions can be obtained from the following equation [12]:

$$I^M = I_{SC}^M\left[1 - \exp\left(\frac{V^M - V_{OC}^M + I^M R_S^M}{V_T^M}\right)\right] \quad (4)$$

Unfortunately, the sentence ends abruptly and the equation is not fully provided. If you need further assistance with completing the translation or understanding specific parts, feel free to ask!

Power System Technology
ISSN:1000-3673
Received: 06-04-2024 Revised: 15-05-2024 Accepted: 28-06-2024

Various variables in the above equation are derived as follows:
The short-circuit current of the module

$$I_{SC}^{M} = N_{PM} * I_{SC}^{C}$$

The open-circuit voltage of the module

$$V_{OC}^{M} = N_{SM} * V_{OC}^{C}$$

The equivalent parallel resistance of the module

$$R_{S}^{M} = \frac{N_{SM}}{N_{PM}} * R_{S}^{C}$$

The equivalent thermal voltage in the module

$$V_{T}^{M} = V_{SM} * V_{t}^{C}$$

$$V_{t}^{M} = \frac{mkT^{C}}{e}$$

The ideality factor \(m \) in the p-n junction significantly influences the characteristics of the photovoltaic module as depicted in the characteristic curve.
Module specifications manufactured by producers are usually tailored for specific conditions, such as nominal or standard conditions, as listed in the table below:

Table 1: Standard and Nominal Conditions for Photovoltaic Modules

Standard Conditions	Nominal Conditions
Irradiance ($G_{a,o} = 1000$) W/m²	Irradiance ($G_{a,o} = 800$) W/m²
Cell Temperature ($T_{P}^{C} = 25$ °C)	Reference Ambient Temperature ($T_{ref}^{a} = 25$°C)
	Reference Cell Temperature ($T_{ref}^{C} = 25$°C)

In standard test conditions (STC), which refer to standard irradiance and temperature, the parameters of short-circuit current of the module, open-circuit voltage of the module, and maximum power of the module ($P_{max,o}^{M}$) are measured.
In nominal conditions, parameters such as reference irradiance ($G_{a,ref}$), reference ambient temperature ($T_{a.ref}$), and reference cell temperature are measured.
The general algorithm for calculating the PV module current under specified operating conditions ((V^{M}, T_{a}, G_{a}) is as follows:
- NSM: Number of cells in series
- NPM: Number of cells in parallel

Power System Technology
ISSN:1000-3673
Received: 06-04-2024 Revised: 15-05-2024 Accepted: 28-06-2024

- IM: Module short-circuit current
- VM: Module open-circuit voltage
- FF: Fill Factor
- a: Short-circuit current temperature coefficient
- C4: Cell temperature coefficient of power
- C1: Voltage temperature coefficient of power
- β: Voltage temperature coefficient
- VMPP and IMPP: Voltage and current at maximum power point (MPP) of the module under standard conditions.

Next step is to determine the characteristics of cell parameters under operating conditions (V^M, T_a, G_a). Therefore, the short-circuit current of a solar cell, ISC, is calculated based on its linear dependency on the environmental temperature:

(9) $I_{SC}^C = C_1 * G_a$

where:

- \(I_{SC} \): Short-circuit current of the solar cell
- \(C_4 \): Coefficient related to the dependence on the environmental temperature
- \(G_a \): Irradiance in the operating conditions

Afterwards, the fill factor (FF), open-circuit voltage (VOC,O), and series resistance (RT,D) are determined using the following equations:

$$FF = \frac{V_{OC,O} - I_N(V_{OC,O}+0.72)}{V_{OC,O}} + 1 \quad (5)$$

$$FF_O = \frac{P_{max}^C}{(v_{OC}^C, I_{OC}^C)} \quad (6)$$

$$r_S = 1 - \frac{FF}{FF_O} \quad (7)$$

$$R_S^C = r_s * (\frac{v_{OC}^C}{I_{SC}^C}) \quad (8)$$

Parameters such as \(C_4 \) are directly related to the environmental irradiance and temperature. The operational temperature of cells, \(T_C \), is exclusively dependent on environmental irradiance and temperature:

$$T^C = T_a + C_2 G_a$$

where:

- T^C:Operational temperature of cells
- \(T_a \): Ambient temperature

Power System Technology
ISSN:1000-3673
Received: 06-04-2024 Revised: 15-05-2024 Accepted: 28-06-2024

- \(C_1 \): Approximately \(5450 \, \text{cm}^{-1} \cdot \text{W}^{-1} \cdot \text{m} \)
The short-circuit current of the module also depends on cell temperature, given by:

$$(12)\ I_{SC}^{M} = C_1 * N_{PM} + a(T^C - 25)$$

The open-circuit voltage varies directly with cell temperature and logarithmically with environmental irradiance. Thus, the relationship is:

$$V_{OC}^{M} = \frac{1}{N_{SM}} * (V_{OC,O}^{M} + \beta(T^C - T_O^C) + C_r(\log(G_a + 1) - \log(G_{a,o})))$$

Constants \(C_r \) and \(\beta \) are available in manufacturer catalogs, otherwise obtainable from V-I module characteristics typically found in all catalogs.
The presence of the number 4 inside \(\log(G_a + 4) \) ensures that the logarithm value does not become infinite when \(G_a \) approaches zero.
The thermal voltage of the cell is derived from:

$$(14)\ V_t^c = \frac{mk(273+T^C)}{e}$$

Once these steps are completed, the calculation steps for photovoltaic module under operating conditions are as follows:

$$(15)\ I^M = N_{PM} * I_{SC}^S * [1 - exp((V^M - N_{SM}V_{OC}^C + I^M R_S^M)/(V_T^M)]$$

Most PV modules have relatively low direct current voltage levels, but with advancements in PV cell technology and the inclination towards single-stage systems and MIC structures, there is a trend towards higher DC voltage modules, often referred to as high-voltage modules (Amiri, 2010).

Methods for Predicting Temperature

As discussed in previous sections, temperature plays a crucial role in solar cells, influencing both economic considerations and energy estimation from photovoltaic (PV) cells. The main objective of this section is to review methods that can calculate module temperature with high sensitivity and minimal error using simple calculations.

Power System Technology
ISSN:1000-3673
Received: 06-04-2024 Revised: 15-05-2024 Accepted: 28-06-2024

Several correlation coefficients have been examined by Cokun et al. (2015) using real data from a solar power plant to evaluate the relationship between PV cell temperature, ambient temperature, solar irradiance, and wind speed.

In real-world conditions, the results for correlation coefficients vary significantly. These discrepancies in temperature correlations with actual data are determined by changes in irradiance. Adjusted virtual correlations and 41 new correlations have been proposed. These correlation equations can easily be used for practical calculations of solar cell system temperatures.

Here, we will examine methods based on ambient temperature (Tambiant) and irradiance (Irradiance) for estimating cell temperature (Cokun et al., 2015).

Review of Major Methods for Estimating Solar Cell Temperature

In this section, we will review the most important methods for estimating solar cell temperature, comparing their respective errors and performance against each other.

Here is the translated and organized version of the additional text:

Temperature Prediction Methods

Parameters and Frequency Error

The parameters of the model are \(a, b, c, d \). \(E_{\text{Frequency}} \) refers to the virtual or absolute frequency correlation error.

Calculation Methods for Temperature Prediction

These models are clearly derived using mathematical equations to predict PV module temperatures directly.

MAE: Mean Absolute Error

$$MAE = \frac{1}{N}\sum_{i=1}^{N}\left|T_{Back,recorded} - T_{Back,predict}\right|$$

Coskun Method

Coskun proposed the following correlation for calculating the temperature of a silicon module \(T_{\text{Back}} \) (Coskun et al., 2016):

$$T_{Back} = 1.14 * (T_a) + \ 0.01 * (G_T - 500) - V_W^{0.8}$$

This correlation was tested, and the results are shown in Figure 0. The mean absolute error for this method is 4.0 degrees Celsius. \(WV \) represents wind speed.

Power System Technology
ISSN:1000-3673
Received: 06-04-2024 Revised: 15-05-2024 Accepted: 28-06-2024

Mondol Method 2

Mondol proposed the following correlation for module temperature \(T_{\text{Cadk}} \) (Mondol et al., 2015):

$$T_{Back} = T_a + 0.031 * G_T - 0.058$$

This correlation is for wind speeds above 4 meters per second with a constant coefficient for heat loss. This correlation was tested, and the results are shown in Figure 1. The mean absolute error was calculated to be 0.00 degrees Celsius.

Mondol Method 1

Mondol proposed another correlation for module temperature \(T_{\text{Cadk}} \) (Mondol et al., 2015):

$$T_{Back} = T_a + 0.031 * G_T$$

This correlation is also for wind speeds above 4 meters per second with a constant coefficient for heat loss. This correlation was tested, and the results are shown in Figure 1. The mean absolute error was calculated to be 4.0 degrees Celsius.

Rose and Smockler Method

Rose and Smockler proposed the following correlation for module temperature \(T_{\text{Cadk}} \):

$$T_{Back} = T_a + 0.035 * G_T$$

When wind speed reaches 4 meters per second, it is accompanied by a heat loss coefficient. This correlation was tested, and the results are shown in Figure 0. The mean absolute error was calculated to be 4.411 degrees Celsius.

Below are the graphs related to these correlations, showing the actual data and the values obtained from the provided functions, which can be observed and compared.

In the charts below, the correlation between the measured and estimated temperatures, as well as the distribution for each of these methods, can be seen and compared with each other.

Power System Technology
ISSN:1000-3673

Received: 06-04-2024 Revised: 15-05-2024 Accepted: 28-06-2024

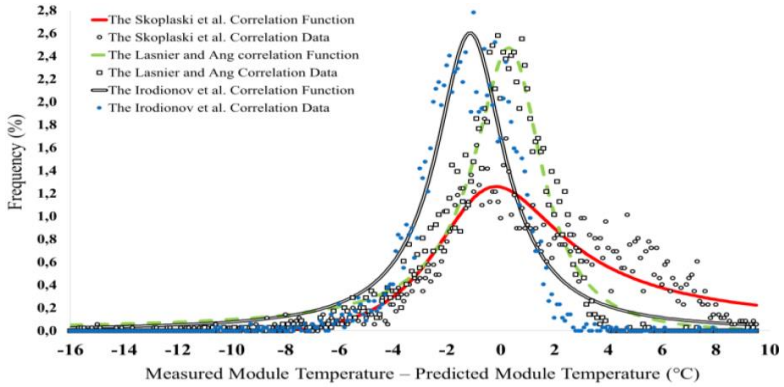

Figure 2: Correlation Graph Between Temperatures Using the Irodionov, Lansier, and Ang Methods

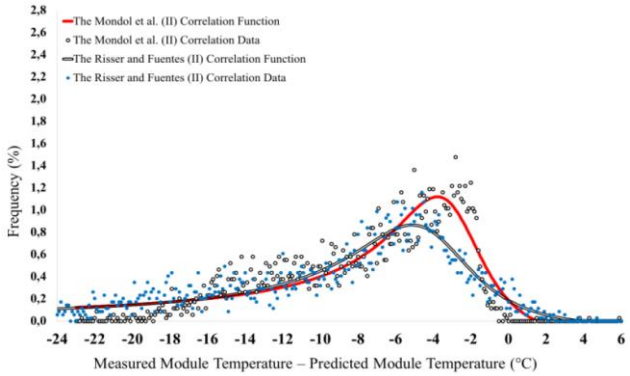

Figure 3: Correlation Graph Between Temperatures Using the Mondol 2 and Rose Methods

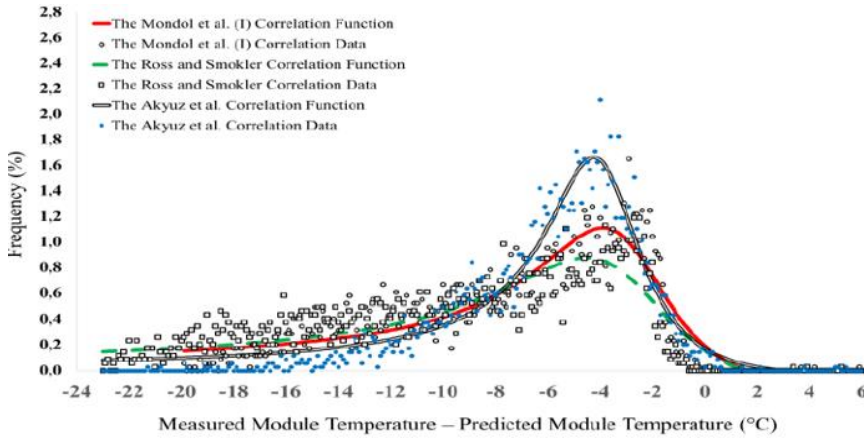

Figure 4: Correlation Graph Between Measured and Predicted Temperatures Using the Mondol 1 and Rose & Smookler Methods

Power System Technology
ISSN:1000-3673
Received: 06-04-2024 Revised: 15-05-2024 Accepted: 28-06-2024

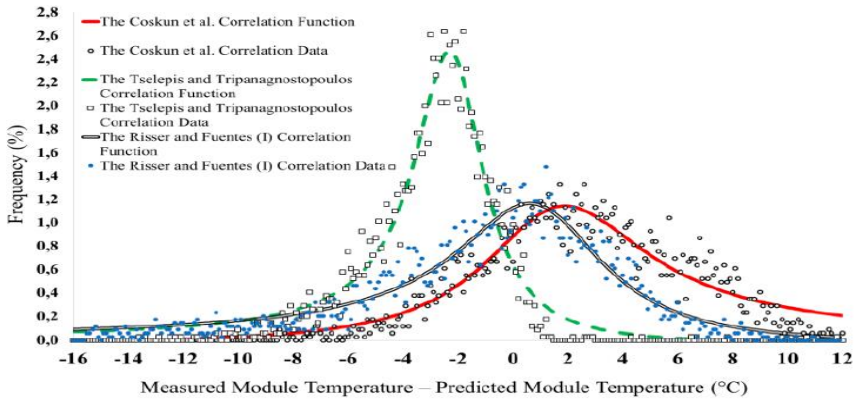

Figure 5: Correlation Graph Between Measured and Predicted Temperatures Using the Tselepis and Tripanagnostopoulos Methods

Temperature Correction

In this section, we address the correction of the correlations discussed in the previous section and present new equations with lower errors.

MRSSI Method

The correlations by Mondol 1 and 2, Rose, Smookler, Scott, and Irodionov have been corrected and are referred to as the MRSSI method. This method proposes the following formula for calculating the module temperature:

$$T_{Back} = T_a - 1.52567 + 0.01981336 * G_T - 0.000003451 * G_T^2$$

This corrected correlation was tested and shown in Figure 1-0. The mean absolute error of this method is calculated to be 1.04 degrees Celsius (Coskun et al., 1541).

LT Method

The correlations by Lansier and Ang, combined with Tselepis and Tripanagnostopoulos, have been revised and renamed as the LT method. This correlation is proposed with the following formula for the sample temperature \(T_{\text{Back}}\):

$$T_{Back} = 1.14 * T_a - 3.101 + 0.01806 * G_T - 0.0000042758 G_T^2$$

This correlation was tested, and the results are shown below. The mean absolute error is 1.14 degrees Celsius. The graph for the corrected equations of this correlation is presented below (Coskun et al., 1541).

Power System Technology
ISSN:1000-3673
Received: 06-04-2024 Revised: 15-05-2024 Accepted: 28-06-2024

Figures

Figure 1-0: Mean Absolute Error for MRSSI Method

This figure shows the comparison of the calculated and actual temperatures using the MRSSI method. The mean absolute error is represented as 1.04 degrees Celsius.

Figure 2-0: Mean Absolute Error for LT Method

This figure shows the comparison of the calculated and actual temperatures using the LT method. The mean absolute error is represented as 1.14 degrees Celsius.

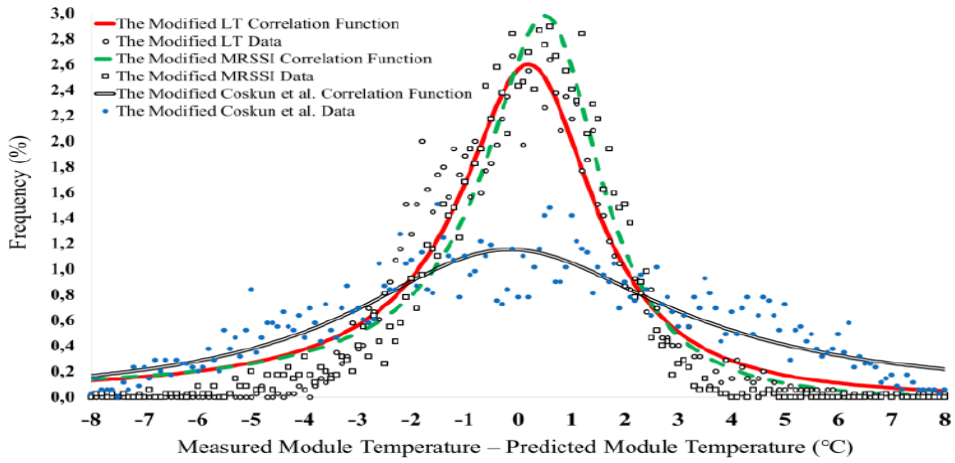

Figure 6: Corrected Correlations for PV Temperature Estimation in LT and MRSSI Methods

The mean absolute error rate ranged from 1.42°C to 1.44°C for the correlation methods. Based on these results, the Lansier and Ang correlations exhibited the best performance among all correlations. The corrected MRSSI and LT methods can be easily used to predict PV module temperature using the single parameter of total solar irradiance and ambient temperature, with less error than other methods.

Implementing a Better Method for Achieving Optimal Output from Neural Networks

We aim to use MLP neural networks, with the following algorithm and 3 inputs:

- Ambient temperature
- Solar irradiance
- Time (in hours, on a smaller scale, seconds)

We will train the neural network to output the current and future panel temperature:

- Current panel (cell) temperature

Power System Technology
ISSN:1000-3673
Received: 06-04-2024 Revised: 15-05-2024 Accepted: 28-06-2024

- Future panel temperature

If this output (panel temperature using temperature and irradiance inputs) has high accuracy and low error (less than 1°C), it can outperform all mathematical estimators mentioned above. Additionally, this network can predict the cell temperature for the next moment, whereas mathematical estimators only respond to the immediate temperature and irradiance.
First, we will train the output in a single-layer hidden network and analyze the results for different neuron counts.
Although time does not directly affect the panel temperature (the main factors are ambient temperature and irradiance), time is included as an input factor because irradiance and ambient temperature are functions of time. Thus, we can use time as an input to further predict cell temperature.
We will start with a hidden layer containing 45 neurons. The next figure will show the specifications and values of the inputs and targets in a table

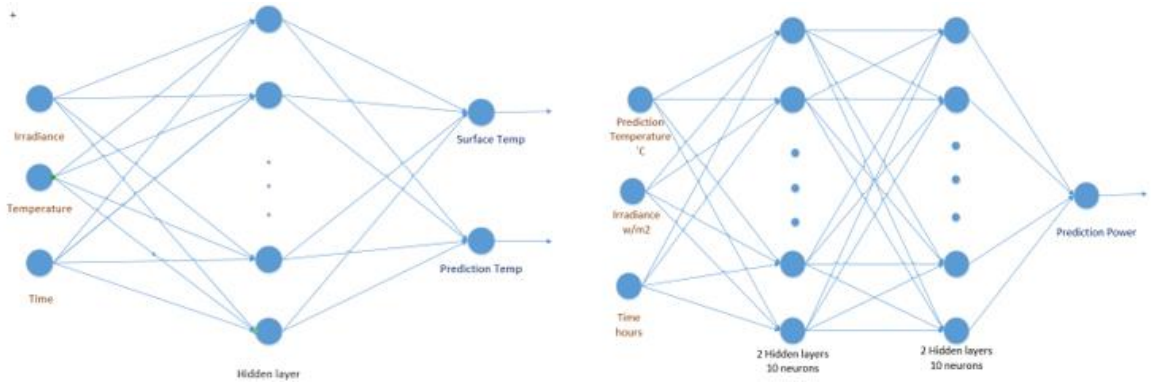

Figure 7: Proposed Neural Network for Estimating Cell Surface Temperature and Predicting Future Temperature and Power

In this network, a hidden layer with 45 neurons each has been used to achieve better results.

Part One:
The input data includes:
- Time
- Irradiance
- Ambient temperature

Power System Technology
ISSN:1000-3673
Received: 06-04-2024 Revised: 15-05-2024 Accepted: 28-06-2024

The output is the estimated cell temperature by the following network:
A neural network with the trainlm training function or Levenberg-Marquardt backpropagation training function is used in this part.
The network consists of three hidden layers with 45, 45, and 30 neurons, respectively, and it is trained using the fitnet function. The network is named net, and the general form is:
\[\text{net} = \text{fitnet(hiddenLayerSize,trainFcn)} \]
- 15% of the data is used for training
- 40% for validation
- 40% for testing

Part Two:
The proposed neural network for power estimation is presented:
The output from the first part (estimated cell temperature) is used as an input for this part. The inputs are:
- Time
- Irradiance
- Estimated temperature from the previous stage

The output of this part, and the overall network, is the maximum power output estimated by our network.
In this part, a neural network with the trainlm training function or Levenberg-Marquardt backpropagation training function is also used.
The network consists of three hidden layers, each with 45 neurons, and is trained using the fitnet function. The network is named net4, and the general form is:
\[\text{net4} = \text{fitnet(hiddenLayerSize,trainFcn)} \]
- 15% of the data is used for training
- 40% for validation
- 40% for testing

Tables 1 and 2, taken from [Mostapha et al., 2012], were used for training the neural network.
- Columns 1, 2, and 4 are our inputs
- Column 3 is the output or target

The network's output should be close to these target values to demonstrate high accuracy and .correlation between inputs and outputs

Power System Technology
ISSN:1000-3673
Received: 06-04-2024 Revised: 15-05-2024 Accepted: 28-06-2024

Table 2: Solar Cell Temperature Estimation Table

Time (H)	Irradiation (W/m²)	Module Temp. (°C)	AmbientTemp. (°C)	Estimated Cell Temp. (°C)
06:00	0	15,46	12,00	15,64
06:30	7,55	15,85	12,80	16,68
07:00	22,23	16,93	13,20	17,39
07:30	36,20	18,80	14,50	19,12
08:00	47,56	20,16	15,50	20,46
08:30	59,5	21,55	16,50	21,81
09:00	70,76	22,80	18,10	23,83
09:30	101,50	25,45	18,70	25,05
10:00	88,50	25,80	20,00	26,30
10:30	100,85	27,25	20,70	27,32
11:00	168,50	30,40	21,90	29,87
11:30	250,15	33,20	22,20	31,64
12:00	397,00	43,10	22,70	34,78
12:30	149,95	40,40	23,00	30,80
13:00	477,33	40,60	23,60	37,21
13:30	732,75	53,20	24,00	42,14
14:00	835,37	60,33	24,30	44,28
14:30	881,05	60,95	24,30	45,08
15:00	922,87	62,16	24,40	45,92
15:30	901,75	52,70	25,00	46,24
16:00	704,13	57,76	26,00	43,92
16:30	935,50	61,30	25,70	47,63
17:00	907,53	60,70	25,20	46,57
17:30	512,00	52,70	25,50	39,99

.In the following table, the estimated power values of the panel are also displayed in tabular form

Table 3: Estimated Power from Solar Cell at Various Times and Cell Temperatures

Time (H)	Back Surface Temperature (°C)	Estimated Power (W)	Measured Power (W)
06:00	15,46	0,00	0,00
06:30	15,85	9,66	0,00
07:00	16,93	28,45	0,00
07:30	18,80	46,33	0,00
08:00	20,16	60,87	0,00
08:30	21,55	76,15	0,00
09:00	22,80	90,57	100,00
09:30	25,45	129,91	105,21
10:00	25,80	113,27	110,48
10:30	27,25	129,08	149,43
11:00	30,40	215,67	197,73
11:30	33,20	320,18	211,22
12:00	37,10	508,15	530,04
12:30	40,40	191,93	250,00
13:00	40,60	610,97	650,39
13:30	53,20	937,91	803,70
14:00	60,33	1069,26	890,91
14:30	60,95	1127,73	915,38
15:00	62,16	1181,26	858,81
15:30	52,70	1154,23	920,22
16:00	57,76	901,27	860,58
16:30	61,30	1197,30	915,36
17:00	60,70	1161,62	816,80
17:30	52,70	655,35	410,17

Power System Technology
ISSN:1000-3673
Received: 06-04-2024 Revised: 15-05-2024 Accepted: 28-06-2024

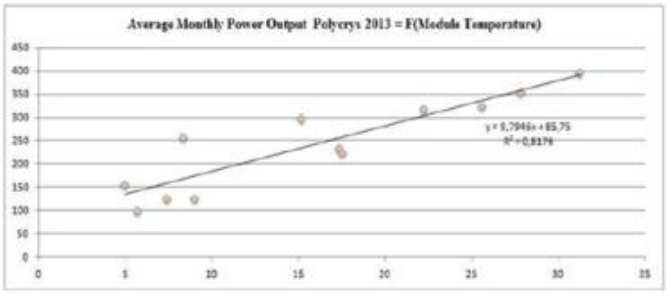

a. Power Output of the PV system and back surface temperature in 2013.

196 It should be noted that the cells' temperature is close to the STC conditions.

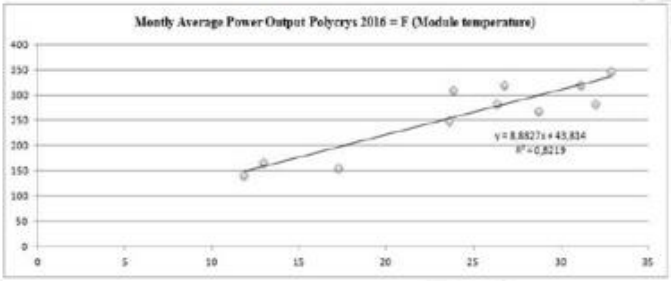

b. Power Output of the PV system and back surface temperature in 2016.

197 Figure 11, is a representation between experimental and estimated values to irradiation
198 level for year 2016.

Figure 8: PV System Output Power for the Years 2113 and 2116

This power and temperatures are for a sample of polycrystalline photovoltaic systems, which are widely used in today's market and have gained significant volume.

The work done here with the neural network is to predict the cell temperature accurately using the available data, and then derive the output power from it, yielding several important results:

This intelligent network, if it has low error in its testing phase, can show us the maximum power by providing time, temperature, and irradiance (under any conditions), offering two advantages:

a) At any moment, it can easily indicate the maximum power without oscillation and without knowing the specific voltage and current.

b) With low error and high correlation, it can perform better than formulaic methods used for estimating cell temperature and power output, particularly those derived from this article's data, providing outputs that are closer and easier to compute.

Initially, I implemented the equation provided in this article, determining their correlation and error for estimated temperature and power using the formulas presented:

Power System Technology
ISSN:1000-3673
Received: 06-04-2024 Revised: 15-05-2024 Accepted: 28-06-2024

$$T_c = 30.006 + 0.0175(\varphi - 300) + 1.14(T_a - 20)$$

The coefficient and correlation between the article's equation and the measured value in cell surface temperature are equal to:

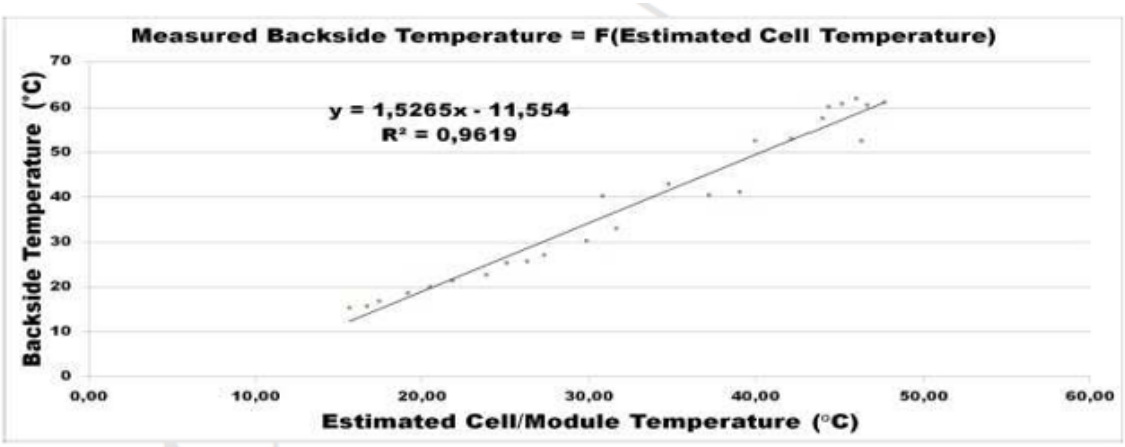

Figure 9: Coefficient and Correlation between the Equation of this Article and Measured Values ((Mostapha et al. 2012))

However, the article ((Mostapha et al. 2012)) does not specify which year this correlation pertains to. The correlation between the temperature derived from the equation and the measured cell surface temperature is 0.4442 for the year 1542, as shown in the figure along with the error values in temperature and power in terms of MSE and RMSE.
The power equation provided in the article is:

The coefficient and correlation between the article's equation and the measured output power for the year 1542 are:

$$P_{calculated} = 1.2161\ P_{measured} + 5.2345,$$
$$R^2 = 96\%.$$

However, this pertains to the year 1542, and for the previous years 1540 and 1541, the value is lower, approximately 0.5401.

Power System Technology
ISSN:1000-3673
Received: 06-04-2024 Revised: 15-05-2024 Accepted: 28-06-2024

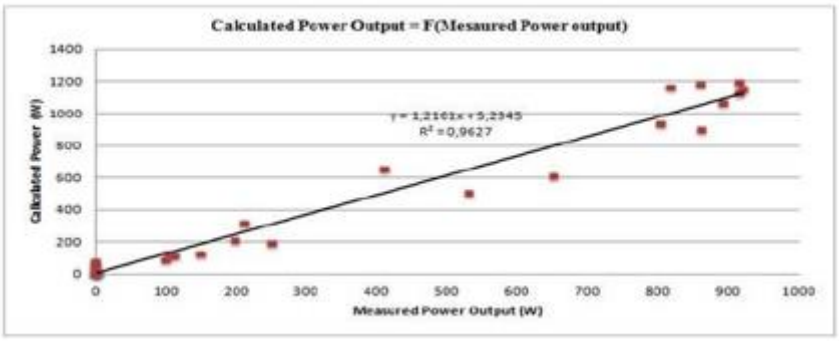

Figure 11: Correlation between measured and predicted values in power output.

As mentioned, if we plot the correlation coefficient \(R \), average error, and RMSE (Root Mean Square Error) for the results of the year 1542 in this paper (Mostapha et al., 2012), although there is no mention of these in the paper, we can implement them using MATLAB functions.

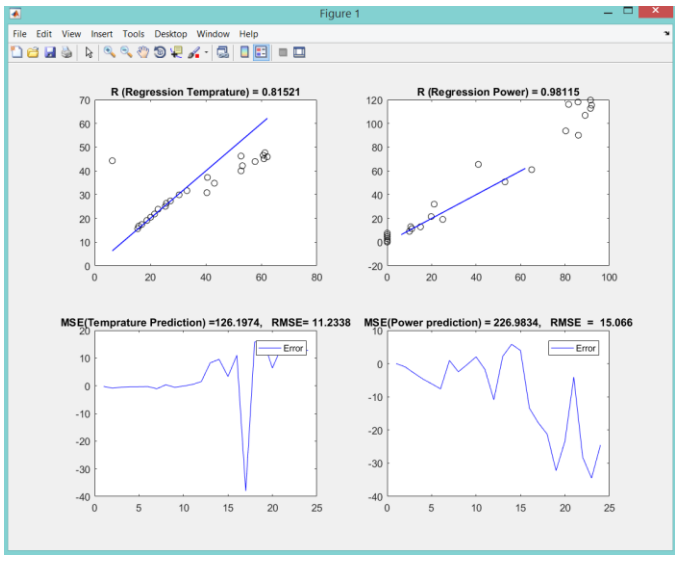

Figure 11: R and RMSE values for the results of the article in the year 2116

We can observe that there is a relatively high MSE and RMSE error for the estimated values of temperature and power of polycrystalline photovoltaic cells. The correlation coefficient for temperature in this year is approximately 0.54014.

After implementing the model proposed in this article, work on neural networks for temperature and power estimation has begun, aiming for our results to surpass those reported in this article.

Power System Technology
ISSN:1000-3673
Received: 06-04-2024 Revised: 15-05-2024 Accepted: 28-06-2024

Working with neural networks offers several advantages, such as:
- It can be applied for all different years with high correlation and significantly lower error compared to this article, which is a valuable outcome.
- Unlike methods like P&O, neural networks can handle severe fluctuations in temperature or irradiance to identify maximum power output more effectively.
I have implemented the neural network with the data from this article, but the results obtained from the neural network are as follows:

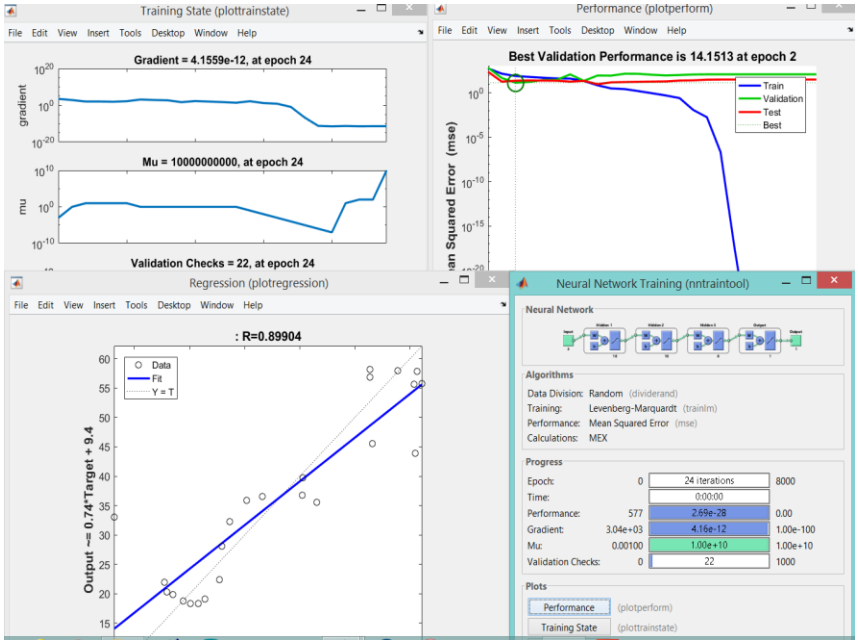

Figure 12: Regression for the desired data for temperature estimation

Although this neural network has been trained to achieve better MSE, RMSE values, and correlation between predicted and measured temperatures in the referenced article, we proceeded by normalizing the neural network and placing the data between 5 to 4, with the largest data being 4 and the smallest data being equal to 5. Then, we trained the network.
In the new network, the error values were significantly lower, which was an excellent outcome. Additionally, its regression and values of mu and sigma were much better compared to the previous network. The regression had reached a level above 4, indicating a very good correlation for the trained network with our target values in both temperature and power. This improved state performs better than all previous networks. However, what mattered more was whether the error

Power System Technology
ISSN:1000-3673
Received: 06-04-2024 Revised: 15-05-2024 Accepted: 28-06-2024

of this new network in estimating temperature and power was better than the normalized network of the reviewed article.

First, below you can see the result of the first part of the neural network which shows the estimated temperature of the photovoltaic cell.

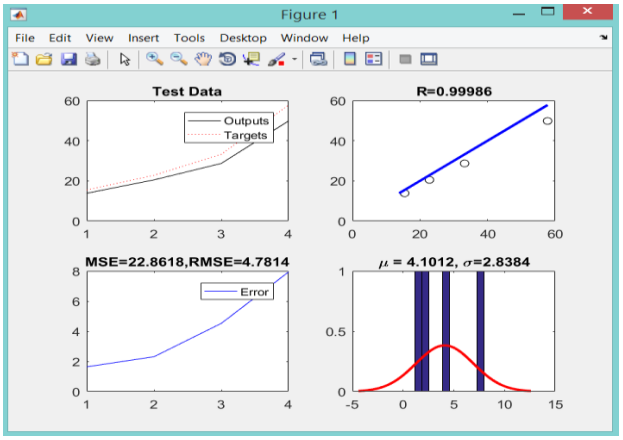

Figure 13: Estimated solar cell temperature and regression with error values using the proposed method.

It can be observed that the regression value is significantly better than that reported in Mostapha et al. (2012), and similarly, its error has also been greatly reduced. Below are the values as reported in the examined article.

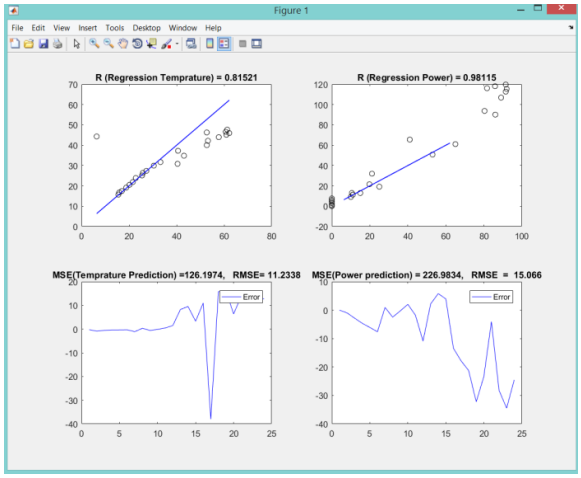

Figure 14: Estimated temperature and power and their errors in Mostapha et al. (2012).

Power System Technology
ISSN:1000-3673
Received: 06-04-2024 Revised: 15-05-2024 Accepted: 28-06-2024

The above values indicate the error and correlation between the estimated and measured temperatures, as well as the estimated and measured output power. With the modifications made in the neural network, the performance metrics, error, and their normal distribution have significantly improved, and the regression value has approached 4. The results of this final section are also presented below for your observation.

We can observe regression, gradient, and the best performance, which are plotted by the neural network itself.

As we can see below, the regression value and the error in estimated output power have significantly improved, and its gradient has also decreased.

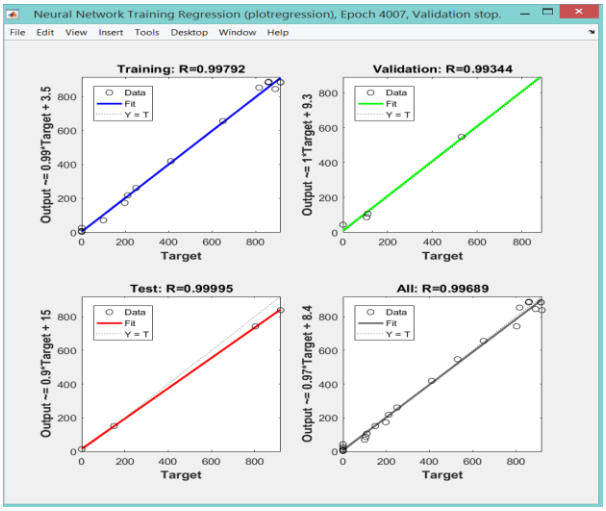

Figure 15: Error value of estimated output power in the proposed network.

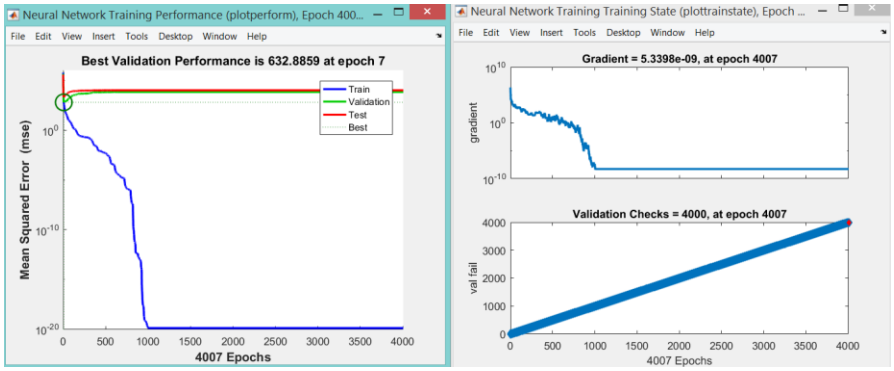

Figure 16: Regression value and validation data.

Power System Technology
ISSN:1000-3673
Received: 06-04-2024 Revised: 15-05-2024 Accepted: 28-06-2024

In this section, using the function we have constructed, we observe our own plots in each scenario for output power, showing significant improvements in results. In this 1 plot, we can see all the trained values and approximate outputs moving close to the target data values.

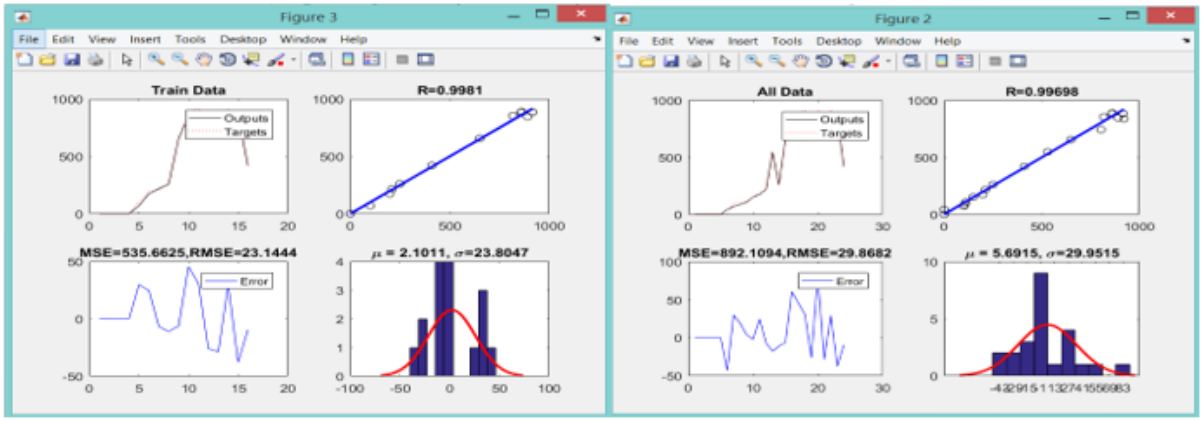

Figure 17: Graph of all data and neural network trained data.

In this section, the results for validation and test data can also be observed.

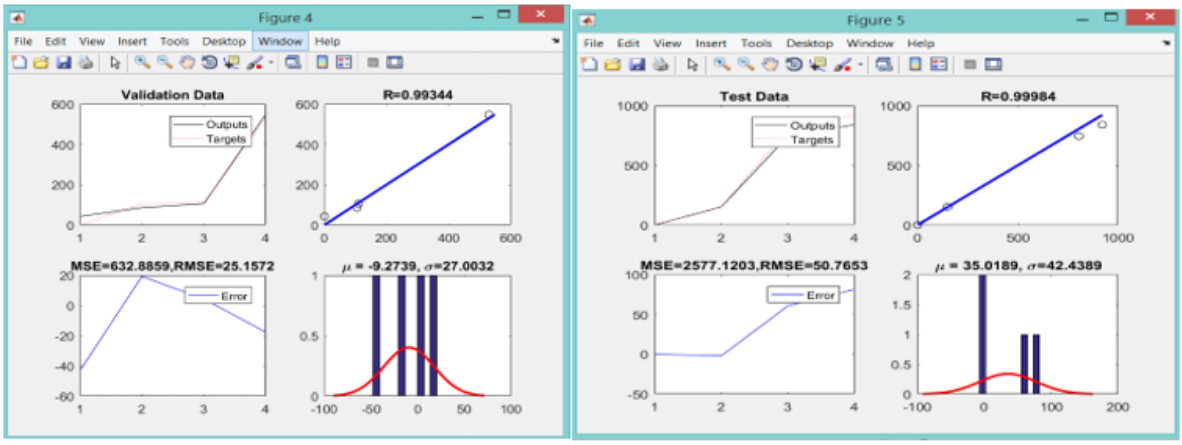

Figure 18: Validation and test data for the proposed neural network.

Conclusion and Discussion:

As observed, initially, a PV model was presented, and the impact of temperature on its various variables was demonstrated. Then, mathematical methods for estimating temperature were introduced, and the error of each was mentioned. Subsequently, a study of a paper containing real data from a solar cell and a mathematical model for estimating temperature and power was

Power System Technology
ISSN:1000-3673
Received: 06-04-2024 Revised: 15-05-2024 Accepted: 28-06-2024

conducted. Finally, the method from this paper, which used neural networks for estimating temperature and power, was compared, and its advantages were observed. We can use this network to estimate temperature with much less error than mathematical models for predicting the temperature and power of a solar cell. Additionally, fuzzy and neural networks can be used for more accurate estimates compared to mathematical methods, and this model can also be used for power plants.

Reference:

[1] A.D. Dhassa, E. Natarajan, P. Lakshmi. (2018). "An Investigation of Temperature Effects on Solar Photovoltaic Cells and Modules," International Journal of Engineering, Vol. 22, No. 11, pp. 1211-1222.
[2] Amiri, Babak. (2010). "Implementation of Fuzzy Control Methods in PV Systems," Master's thesis, Kurdistan University.
[3] Can Coskun, Ugurtan Toygar, Ozgur Sarpdag, Zuhal Oktay. (2012). "Sensitivity Analysis of Implicit Correlations for Photovoltaic Module Temperature: A Review," Journal of Cleaner Energy.
[4] Coskun, C.; Kocyigit, N.; Oktay, Z. (2011). "Estimation of PV Module Surface Temperature Using Artificial Neural Networks," Mugla Journal of Science and Technology, Vol. 2, No. 2, pp. 11-19.
[5] Irodionov, A. E.; Kurenkova, V. A.; Potapov, V. N.; Strebkov, D. S. (1992). "Choice of Resistance for Elements of Photovoltaic System's External Switching," Geliotechnika, Vol. 21, pp. 19-21.
[6] Jiyong Li and Honghua Wang. (2002). "A Novel Stand-alone PV Generation System Based on Variable Step Size INC MPPT and SVPWM Control," December 2002, pp. 1211-1220.
[7] Lasnier, F.; Ang, T. G. (2020). "Photovoltaic Engineering Handbook," CRC Press, New York.
[8] Mohammad Raye Neyini, Mohsen; Jalili, Mojtaba; Bastani, Saeed; Khamese, Sara. (2011). "Printed Solar Cells: The Inevitable Solution to the Global Energy Crisis," Studies in the World of Color Journal, Vol. 40, No. 1.
[9] Mondol, J. D.; Yohanis, Y. G.; Norton, B. (2002). "Comparison of Measured and Predicted Long Term Performance of a Grid Connected Photovoltaic System," Energy Conversion and Management, pp. 1011-1090.
[10] Mondol, J. D.; Yohanis, Y. G.; Smyth, M.; Norton, B. (2001). "Long-term Validated Simulation of a Building Integrated Photovoltaic System," Solar Energy, pp. 111-121.
[11] Moustapha Ba, Harry Ramenah, Camel Tanougast. (2012). "Forecasting Photovoltaic Energy Output Determination by a Statistical Model Using Real Module Temperature in the Northeast."
[12] Ross, R. G.; Smokler, M. I. (1991). "Flat-plate Solar Array Project Final Report – Volume VI: Engineering Sciences and Reliability," Report DOE/JPL-1012-121.
[13] Sadeghi, Sahar; Jahani, Hossein; Eqbami, Behnam; Sardarmoghaddam, Ahmad. (2010). "A Comparative Review of Various Generations in Solar Cells," First International Conference on Information Technology, Mechanics, Electrical and Engineering Sciences.
[14] Tselepis, S.; Tripanagnostopoulos, Y. (2001). "Economic Analysis of Hybrid Photovoltaic/Thermal Solar Systems and Comparison with Standard PV Modules," Proceedings of the International Conference on PV in Europe, Rome, Italy, October, pp. 2111-2119.